Vanadium adsorption and incorporation at the GaN(0001) surface: A first-principles study

Rafael González-Hernández* and William López-Pérez
Grupo de Física de la Materia Condensada (GFMC), Departamento de Física, Universidad del Norte, A. A. 1569 Barranquilla, Colombia

María Guadalupe Moreno-Armenta
Centro de Nanociencias y Nanotecnología de la UNAM, Km. 107 Carretera Tijuana-Ensenada, Ensenada, Baja California, Mexico

Jairo Arbey Rodríguez M.†
Grupo de Estudio de Materiales (GEMA), Departamento de Física, Universidad Nacional de Colombia, A. A. 5997 Bogotá, Colombia
(Received 16 October 2009; revised manuscript received 12 April 2010; published 5 May 2010)

We have carried out first-principles spin-polarized calculations in order to study the energetics and electronic structure of vanadium adsorption and incorporation on GaN(0001)-2×2 surface using density-functional theory within a plane-wave ultrasoft pseudopotential scheme. It was found that V atoms preferentially adsorb at the T4 sites at low and high coverages (from 1/4 up to 1 monolayer). In addition, calculating the relative surface energy of several configurations and various V concentrations, we constructed a phase diagram showing the energetically most stable surfaces as a function of the Ga chemical potential. Based on these results, we found that incorporation of V adatoms in the Ga-substitutional site is energetically more favorable compared with the adsorption on the top layers. Our calculations show that the vanadium incorporation is most favorable under a nitrogen environment, in agreement with recent experimental results.

DOI: 10.1103/PhysRevB.81.195407 PACS number(s): 68.43.Bc, 68.35.Md, 71.15.Mb, 73.20.At

I. INTRODUCTION

Gallium nitride (GaN) is one of the wide direct band-gap semiconductors, which has a broad range of potential applications for optoelectronic and high-power electronic devices. Light-emitting diodes are a commercial reality due to an intense activity in the recent past years.[1] Its high thermal conductivity also opens new routes in high-temperature and high-power electronic devices,[2,3] such as metal-semiconductor field-effect transistors, high electron mobility transistors, and heterojunction bipolar transistors.[4,5] Additionally, high Curie temperatures and room-temperature ferromagnetism have been predicted in GaN doped with transition-metal (TM) elements, which, in principle, opens a door to semiconductor-based spintronic applications.[6,7]

The electronic and magnetic properties of transition metals in GaN regained prominence due to potential application for the growth of high-resistivity GaN substrate material and for dilute magnetic semiconductors.[8–10] In particular, the 3*d* TM elements can be expected that substitute Ga atoms during crystal growth. The knowledge of their associated deep defects is very important for the development of new kinds of devices such as electro-optic switches, ultrasensitive magnetic field sensors, and quantum-mechanism-based logic for high-speed computation.[11] Additionally, the incorporation of TMs (Cr, Fe, and V) produces luminescence in the infrared region.[12,13]

TMs elements have been introduced to bulk GaN using several techniques, such as ion implantation; for example, when Co or Cr is implanted in GaN, a ferromagneticlike behavior is observed. In contrast, when V is implanted in GaN, a paramagnetic order is exhibited.[14] Other studies of GaN:V layers permit us to conclude that the behavior is paramagnetic, including when the layers are implanted with Mn and Cr.[15] However, an antiferromagnetic coupling of the 3*d* TM ions was observed but the samples presented no ferromagnetic order. Such results show that a lot of research on GaN doped with V, Cr, Co, and Mn is necessary, and the study of the interaction between a V atom with Ga (or N) atoms on the GaN surfaces can lead to a deeper knowledge of the problem.

Theoretical studies of the pressure effect on the electronic and magnetic properties of $Ga_xV_{1-x}N$ have shown that the spin magnetic moment per cell (SMMC) seems to change abruptly at a certain critical pressure.[16] Similar studies on GaN surfaces have shown the importance of such research because a Ru/GaN Schottky diode was fabricated;[17] therefore such a system is of technological interest for use in ultrahigh-power devices. A study of GaN(0001):Ru shows that the Ru adatom is adsorbed at the T4 position and it presents a 0.61 eV surface diffusion energy barrier.[18]

Despite progress in growing high-quality material for device fabrication, an understanding of the fundamental growth mechanisms of GaN is still in its infancy. Even the structure of clean and adsorbate covered surfaces and the mechanisms of incorporation and diffusion of adatoms are not well comprehended. An understanding of these mechanisms is important for obtaining a deeper insight into the relevant growth mechanisms on an atomic scale and for improving growth in a controlled fashion.[19,20] In this paper, we perform first-principles spin-polarized calculations for the adsorption and incorporation of vanadium adatom on the GaN(0001) surface with different V-doped configurations, using density-functional theory (DFT) within a plane-wave ultrasoft pseudopotential scheme. We focus on the technologically most relevant GaN(0001) surface, which is the polarity observed during metal-organic chemical vapor deposition (MOCVD) of GaN on sapphire as well as molecular beam epitaxy on Si-face SiC.[21,22] Based on the fact that (2×2) surface reconstruction is one of the most commonly ob-

TABLE I. Calculated and experimental structural parameters and cohesive energies (E_o) of bulk wurtzite GaN, α gallium, N_2 molecule, and bulk bcc vanadium.

	a (Å)		b (Å)		c (Å)		Bond length (Å)			E_o (eV)	
Structure	Calc.	Expt.	Calc.	Expt.	Calc.	Expt.	Calc.		Expt.	Calc.	Expt.
GaN (bulk)	3.218	3.190[a]			5.242	5.189[a]	d_{GaN}	1.976	1.956[a]	8.54	9.058[b]
							d_{GaN}	0.644	0.638[a]		
α-Ga (bulk)	4.52	4.51[c]	4.53	4.52[c]	7.66	7.64[c]	d_{GaGa}	2.50	2.44[c]	2.72	2.81[c]
N_2 (molecule)							d_{NN}	1.114	1.098[d]	4.84	4.91[e]
V (bulk)	3.00	3.02[f]					d_{VV}	2.60	2.62[f]	5.28	5.31[f]

[a]Reference 30.
[b]Reference 31.
[c]Reference 32.
[d]Reference 33.
[e]Reference 34.
[f]Reference 35.

served on GaN(0001),[23,24] we chose a GaN(0001)-2×2 surface supercell in the calculations.

II. COMPUTATIONAL METHODS

The total-energy and electronic-structure calculations were performed using the first-principles pseudopotential method in the framework of the spin DFT. Exchange and correlation effects were treated with generalized gradient approximation implemented in the Perdew-Burke-Ernzerhof functional.[25] Ultrasoft pseudopotentials were employed,[26] wherein the 3*d* states for Ga and V were included as valence electrons. The calculations were performed using the QUANTUM-ESPRESSO simulation package.[27] The electron wave functions were expanded in plane waves up to a cutoff energy of 30 Ry and a cutoff of 300 Ry for the charge density. A gamma centered grid of $3\times3\times1$ k point for the hexagonal lattice has been used to sample the irreducible Brillouin zone in the Monkhorst-Pack special scheme.[28] Methfessel-Paxton smearing technique with a smearing width of 0.02 Ry was adopted.[29] These parameters ensure a convergence better than 5 meV for the total energy.

The surface calculations were performed using a slab geometry consisting of four GaN(0001) bilayers of which the lowest bilayer was fixed in the bulk configurations, and minimizing the total energy with respect to the positions of all of the atoms in the three uppermost GaN bilayers (plus V adatom). Relaxations in the third bilayer were negligible, indicating that a sufficiently large slab was employed. The GaN(0001)-2×2 surface unit cell (without adatoms) included eight wurtzite GaN unit cells (two in the [0001] direction and four in the planes parallel to the surface). Undesirable charge transfer was prevented by the passivating of the bottom layers by pseudohydrogen atoms. For the Ga-terminated (0001) surface, the 1.25e fractional charges associated with the dangling bonds in the N bottom layer were saturated with pseudohydrogen atoms, each with a fractional charge of 0.75e. The structural optimizations were terminated when the magnitude of the force acting on each ion was less than 1 mRy/bohr. A vacuum thickness of ~10 Å has been used throughout the calculations.

III. RESULTS AND DISCUSSION

A. Vanadium adsorption

Before starting the surface calculations, we first have optimized the structural parameters for GaN in the wurtzite structure, which is the most stable phase of GaN at low temperatures and pressures. The optimized parameters for GaN were used to build the slab for the GaN(0001)-2×2 surface calculations. The lattice parameters, interatomic distances, and cohesive energies for GaN, Ga-bulk, N_2 molecule, and V-bulk are presented in Table I. Gallium has different bulk phases but theoretical and experimental studies have shown that α-Ga (orthorhombic structure) is the most stable phase at room temperature. Vanadium crystallizes in a body-centered-cubic (bcc) crystal structure. The set of calculated structural parameters are in good agreement with experimental values (to within 1%). The cohesive energies of N_2, Ga-bulk, and V-bulk are very close to experimental data (to within 5%). With the values found previously, the calculated GaN heat of formation in wurtzite structure is $\Delta H_f^{GaN}=-0.98$ eV, which agrees with previous calculations and experimental results.[36–38]

The GaN(0001) surface is well known from an experimental as well as theoretical point of view.[21–24,39–42] The equilibrium atomic positions were calculated via structural relaxation of a clean GaN(0001) surface. The structure parameters d_{ad}, d_{12}, and d_{23} characterizing the relaxations of surfaces (clean and with adatom) are introduced in Fig. 1(b). The calculated parameters of structure relaxations for a clean GaN(0001) surface are given in Table II. On the clean Ga-terminated (0001) surface, the topmost GaN bilayer moves outward by 0.03 Å with respect to its ideal bulk position, in agreement with the results reported by Wang *et al.*[42]

For adsorption study, a variety of adatom positions have been investigated in order to determine the most stable structure. There are three different high-symmetry points on the

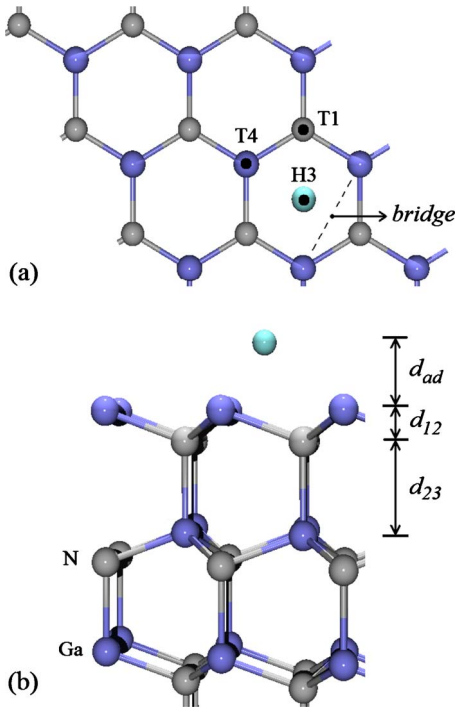

FIG. 1. (Color online) Ball and stick model of the V adatom at the H3 site. The blue balls represent Ga atoms and the gray balls represent N atoms. (a) Top view of the H3, T4, and T1 adsorption sites and (b) side view with the notation used for the interlayer distances.

clean Ga-terminated GaN(0001)-2×2 surface as shown in Fig. 1. A vanadium atom is placed at the T1, H3, and T4 positions and the atomic positions were relaxed. Table II shows the geometric data of the V adatom on the GaN(0001) surface after relaxation, as are defined in Fig. 1(b). The adsorption energies E_{ads} were calculated as the difference between the total energy of the GaN(0001) slab with adsorbed vanadium and the sum of the total energies of the clean surface and the isolated vanadium atom. The bond lengths d_{GaV} were obtained from the average distance between V adatom and nearest Ga surface atoms. The E_{ads} values and bond lengths d_{GaV} are shown in Table II. We can observe than the adsorption of a V adatom at the T4 site is more favorable than the V adsorption at the H3 site. The V adsorption at the T1 position is energetically unfavorable. The E_{ads} value for T4 site is slightly lower than our calculated value for Ga-T4 reconstruction (−3.83 eV). The T4 preference adsorption

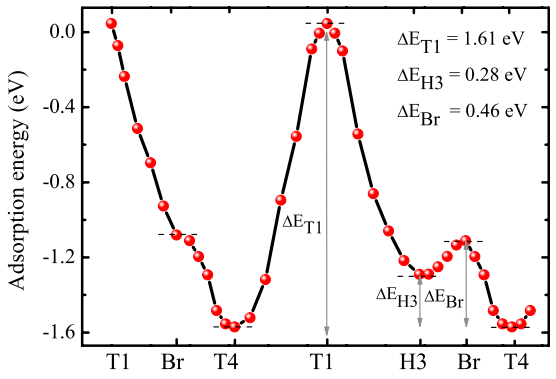

FIG. 2. (Color online) Adsorption energy for vanadium adatom at different sites on GaN(0001)-2×2 surface. The adsorption energy is referred to the cohesive energy of V-bulk.

site for V adatom is the same as that is preferred for Ga adatom.[39]

The diffusion barriers for V adatom have been calculated by plotting the two-dimensional (2D) total-energy surface (TES). The TES was calculated by fixing the adatom laterally and allowing vertical relaxation. Figure 2 shows the TES for several paths through high-symmetry points for the V adatom, such as those that Fig. 1(a) shows. The local minima from Fig. 2 generally provide an ample range of possible stable, or in the event metastable, adsorption sites for the V adatom. The calculations demonstrate that V adatoms avoid the T1 position. Vanadium adatoms prefer to adsorb at the T4 and H3 positions. The TES also gives immediate insight about diffusion barriers and migration paths. Figure 2 is valid for the diffusion of one only V atom on the clean GaN(0001) surface. However, if there were another atom adsorbed on the surface, the diffusion path and diffusion barriers would change. In Fig. 2, the energetically highest site between T4 and H3 is the bridge position. The barrier for the migration from H3 toward T4 is about 0.18 eV and is 0.46 eV for the reverse path. The small energy barriers are an indication of a weak bond of the V adatom and the Ga-top atoms in the GaN(0001) surface. Similar adatom barriers were also obtained for the Ga-Ga bond on this surface.[43]

In order to research the effect of the V monolayer (ML) adsorption on the GaN(0001) surface, we have placed V adatoms at the T4, H3, and T1 positions. Defining the surface coverage (θ_{V}) as the ratio of the amount of adsorbed vanadium adatoms to the ML sites capacity, we have built monolayer coatings with $\theta_{\mathrm{V}}=1/4$, 1/2, 3/4, and 1 ML for the cov-

TABLE II. Calculated structural parameters d_{ad}, d_{12}, and d_{23} introduced in Fig. 1(b), bond length d_{GaV}, adsorption energy E_{ads}, and spin magnetic moment per cell SMMC.

	d_{GaV} (Å)	d_{ad} (Å)	d_{12} (Å)	d_{23} (Å)	E_{ads} (eV)	SMMC (μ_B)
Clean			0.67	2.00		
			0.72[a]	2.01[a]		
V-T4	2.49	1.63	0.79	1.93	−3.71	2.05
V-H3	2.66	1.91	0.85	1.97	−3.43	2.90
V-T1	2.52	2.52	0.81	1.97	−2.10	3.94

[a]Reference 42.

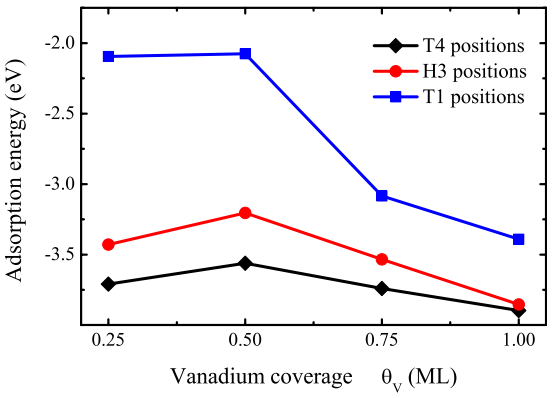

FIG. 3. (Color online) Adsorption energy at the GaN(0001) surface vs coverage for tree high-symmetry sites. The lines are only a guide to eyes.

erage at the GaN(0001)-2×2 surface. In Fig. 3, we plot the adsorption energy (in electron volt per vanadium atom) vs coverage for the high-symmetry positions shown in Fig. 1(a). We have found that the V adatom preferentially adsorbs at T4 sites at low and high coverages (from 1/4 up to 1 monolayers). The preference for the T4 vanadium positions can be attributed to the electrostatic attraction between positively charged V adatom and the negative charged N-top bilayer. In addition, when the coverage varies from 1/4 to 1 ML, the changes in the adsorption energy for V atoms adsorbed at the T4 positions are, at most, around 0.3 eV. This small variation in the adsorption energy is an indication of the weak interaction between V atoms in the adsorbed monolayer. It is shown that the growth of vanadium monolayers on this surface is possible. This fact is interesting from a theoretical point of view and for its technological applications.

B. Vanadium incorporation

In order to investigate the incorporation into a growing layer, we carried out total-energy calculations for vanadium atoms in various configurations. We found that a vanadium atom located in the interstitial positions or N-substitutional sites is unstable. We conclude that in the region close to the Ga-terminated surface, V is mainly found in the Ga-substitutional site. Similar results were found by Bungaro *et al.*[44] and Rosa *et al.*[45] for the Mg and Si incorporation, respectively.

The relative energies of different V-doped configurations are shown in Fig. 4. In this section, a large number of configurations with different amounts of V atoms in substitutional Ga sites were studied and denoted as $(n1/n2/n3/)$, where $n1$, $n2$, and $n3$ are the numbers of substitutional V impurities in the first, second, and third bilayer, respectively, starting from the surface. For example, (2/0/0/) represents the configuration where two V atoms are incorporated in the first bilayer (0.50 ML), and vanadium atoms are not present in the deeper bilayers.

From Fig. 4, it appears that at a 0.25 ML concentration, V prefers to incorporate in the first bilayer. The total energy for V in the second bilayer is very close in energy (about 0.03 eV higher) while the energy further increases by 1.25 eV for

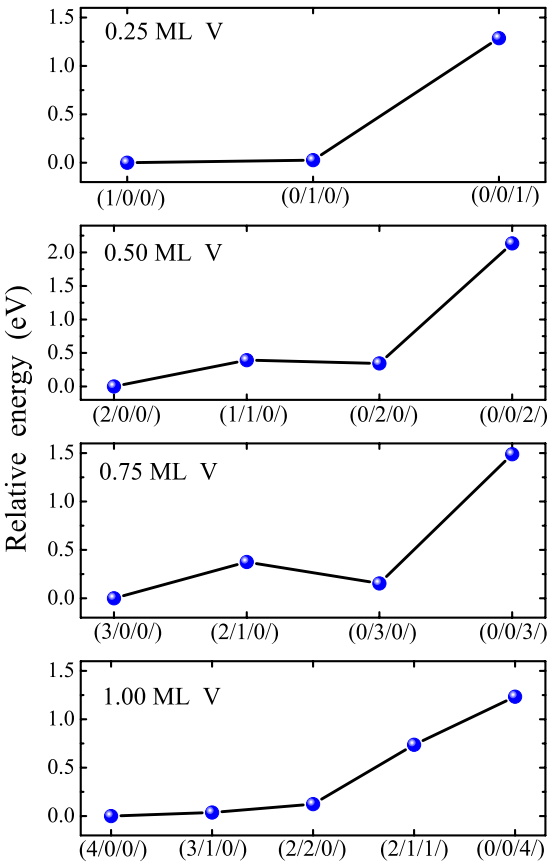

FIG. 4. (Color online) Relative energies of different configurations for V incorporated in the clean GaN(0001) surface. Different configurations are labeled as $(n1/n2/n3/)$, where $n1$, $n2$, and $n3$ are the numbers of incorporated V in the first, second, and third GaN bilayer in a 2×2 supercell. The lines that join the points are only a guide for the eyes.

V in the third bilayer. As the V concentration increases to 0.50 ML, the most stable configuration has all V atoms in the first bilayer but the configurations (1/1/0/) and (0/2/0/) are close in energy, about 0.34 eV and 0.39 eV higher, respectively. As the concentration of incorporated V further increases to 0.75 ML, the (3/0/0/) configuration becomes slightly more stable than the (0/3/0/). At 1.0 ML concentration, the most stable configuration in Fig. 4 is (4/0/0/), configuration (3/1/0/) being, almost degenerate. Therefore, for V incorporation at the GaN(0001) surface, the vanadium atoms prefer one Ga substitution at the top bilayer and there appears to be no migration to the GaN bulk. The preference of the V incorporation in the first bilayer can be due to the vanadium interaction with nitrogen atoms from the GaN to form VN. V-N bond formation is thermodynamically supported because the heat of formation of VN (ΔH_f^{VN}= −2.25 eV) is preferred over that of GaN ($\Delta H_f^{\mathrm{GaN}}$= −1.14 eV).[38] Recently, Pookpanratana *et al.*[46] observed the formation of VN bonds in the GaN interface, which is consistent with the present theoretical results.

C. Surface energy

From total-energy results for the adsorption and incorporation, we found the relative formation energy for

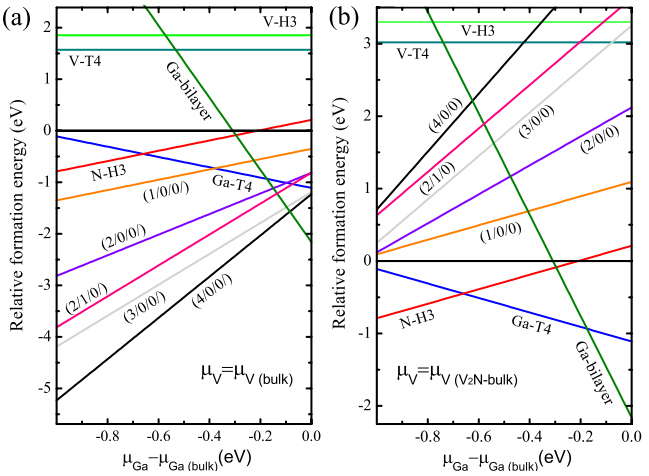

FIG. 5. (Color online) Relative formation energies for possible models of V incorporated and adsorbed at the clean GaN(0001)-2 $\times 2$ surface vs the Ga chemical potential μ_{Ga} in the range $\Delta H_f^{GaN} \leq \mu_{Ga} - \mu_{Ga(bulk)} \leq 0$. V-rich conditions are assumed, i.e., (a) $\mu_V = \mu_{V(bulk)}$ case and (b) $\mu_V = \mu_{V(V_2Nbulk)}$ case. The zero of the energy scale corresponds to the formation energy of the clean GaN(0001) surface.

GaN(0001):V as a function of the gallium chemical potential μ_{Ga}. Because the surface stoichiometry is not the same for all the studied configurations, the formation energies depend on the chemical potential of the atomic species in excess. The relative formation energy E_f is written as[47]

$$E_f = E_{total} - E_{ref} - \Delta n_V \mu_V - \Delta n_{Ga} \mu_{Ga} - \Delta n_N \mu_N, \quad (1)$$

where E_{total} is the total energy of the configuration under consideration, E_{ref} is the total energy of the reference configuration, in this case the clean GaN(0001) surface, μ_i is the chemical potential of the ith species, and Δn_V is the excess or deficit of V atoms with respect to the reference; similar definitions hold for Δn_{Ga} and Δn_N. At equilibrium, the chemical potential of a given species is equal in all phases that are in contact. This can be exploited to impose constraints on the possible equilibrium values. In particular, we assume that the surface is at equilibrium with the GaN bulk so that $\mu_{GaN(bulk)} = \mu_{Ga} + \mu_N$, where $\mu_{GaN(bulk)}$ is the chemical potential of bulk GaN. Another constraint is that the chemical potential of each atomic species must be low enough to avoid the formation of undesirable phases; $\mu_{Ga} \leq \mu_{Ga(bulk)}$ (prevents the formation of Ga droplets), $\mu_N \leq \mu_{N_2(molecule)}$ (prevents GaN decomposition), $\mu_V \leq \mu_{V(bulk)}$, and $\mu_V \leq \mu_{V(V_2Nbulk)}$ (prevent the formation of V and V_2N precipitates, respectively). With the above choices, the relative formation energy is a function of μ_{Ga}. In the thermodynamically allowed range of the Ga chemical potential, we have[48]

$$\mu_{Ga(bulk)} + \Delta H_f^{GaN} \leq \mu_{Ga} \leq \mu_{Ga(bulk)}, \quad (2)$$

where $\mu_{Ga(bulk)}$ is the chemical potential of Ga in bulk phase and ΔH_f^{GaN} is the GaN heat of formation, the lower limit means N-rich conditions, and similarly the upper limit means the Ga-rich condition.

In Fig. 5, the calculated relative formation energies for the more energetically favorable vanadium incorporated and adsorbed configurations at the GaN(0001)-2 $\times 2$ surface are shown as a function of μ_{Ga}. In order to study the high concentration of vanadium atoms, we have chosen two values for the V chemical potential: $\mu_V = \mu_{V(V\text{-}bulk)}$ case [see Fig. 5(a)] and $\mu_V = \mu_{V(V_2N\text{-}bulk)}$ case [see Fig. 5(b)]. In the absence of V, we reproduce the results for the clean GaN(0001) surface reported in Ref. 49. Under moderately Ga-rich conditions, the most favorable reconstruction is the Ga adatom in a T4 position (Ga-T4) while under N-rich conditions, the N adatom in the H3 position is most stable (N-H3). Under extreme Ga-rich conditions, a contracted Ga bilayer reconstruction (Ga bilayer) is energetically most favorable, in good agreement with previous results.[49,50]

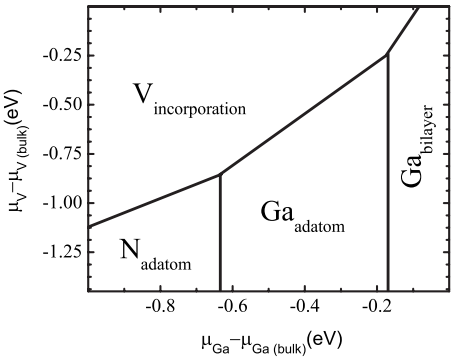

FIG. 6. Phase diagram of the relative stability of the different configurations for the GaN(0001) surface in the presence of V, as a function of the chemical potentials of vanadium and gallium.

In Fig. 5(b), we observe that the N-H3, Ga-T4, and Ga-bilayer models are the most stables structures for the $\mu_V = \mu_{V(V_2N\text{-}bulk)}$ case, this indicates that the V adsorption and incorporation are not energetically favorable on the GaN(0001) surface. However, for the whole range of the chemical potential, V in the Ga-substitutional site is the most stable configuration, strongly favored with respect to on-surface adsorption. In Fig. 5(a), the GaN(0001) surface with four substitutional V atoms at four Ga sites in the first bilayer, configuration (4/0/0/), is found to be most energetically favorable structure. From Fig. 5(a), as the environment becomes progressively more Ga rich, the relative stability of the vanadium incorporated with respect to adsorbed configurations decreases. In extreme Ga-rich conditions, the contracted Ga bilayer becomes the most stable configuration. We found that the growing of GaN:V under a nitrogen-rich environment mainly seems to be most energetically favorable. These results are in agreement with the recent results obtained by Souissi *et al.*[13] for the growing of vanadium-doped GaN samples elaborated by MOCVD.

The relative stability of configurations with variable concentration of the V and Ga adatoms is summarized in the phase diagram shown in Fig. 6. Each region of the phase space is identified by the values of the Ga and V chemical potentials (horizontal and vertical axes, respectively) and is labeled according to the lowest formation energy for the corresponding values of μ_{Ga} and μ_V. From left to right, we have N-rich to Ga-rich conditions, from top to bottom we have V-rich to V-poor conditions; these definitions are related to

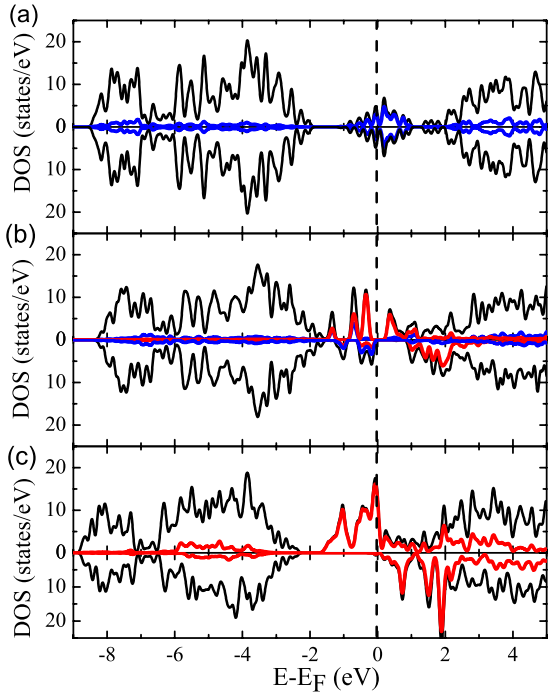

FIG. 7. (Color online) Total DOS for (a) the relaxed clean GaN(0001) surface. Ga-top-layer-projected DOS is also shown (blue line), (b) the V-T4 reconstruction. V adatom and Ga-top-layer projected DOS are also shown (red and blue line, respectively), (c) the configuration (4/0/0/). V-top-layer-projected DOS is also shown (red line). The Fermi level (E_f) is set to 0 eV.

the abundances of the precursors in the environment. For Ga-rich conditions, the phase diagram shows that the most favorable structure is the Ga-bilayer structure. Going toward more N-rich conditions, a surface structure is formed which consists of a V-N layer in the first bilayer (V incorporation). For V-poor conditions, the GaN(0001)-2×2 surface (Ga-T4 and N-H3) reconstruction structures are reproduced.

D. Electronic properties

In Fig. 7(a), we show the density of states (DOS) for the relaxed clean GaN(0001)-2×2 surface. Ga-top-layer-projected DOS is also shown (blue line). The positive and negative DOS values correspond to majority- and minority-spin contributions. We can observe a metallic band due to surface states in the band gap mainly due to the Ga-top-layer atoms, Zywietz *et al.*[20] also found such results. Figure 7(b) shows the DOS for the V-T4 reconstruction. V adatom and Ga-top-layer atoms projected DOS are also shown (red and blue line, respectively). In this case, the surface tries to saturate the dangling bonds thereby reducing the density of states within the fundamental band gap; the surface dangling bonds are saturated by the vanadium adsorption. An energy gap around E_f is presented in both majority and minority DOS. The gap value between the majority-spin component and the minority is different: ~0.5 eV for the majority and ~1.0 eV for the other else spin components. The V-T4 reconstruction results in a semiconducting behavior with a gap of about ~0.4 eV, and two regions of surface states appearing within the band gap. The majority states mainly arise from V-adatom states, and the minority states are occupied from dangling bonds of Ga atoms in the top layer with a low contribution of V-adatom states.

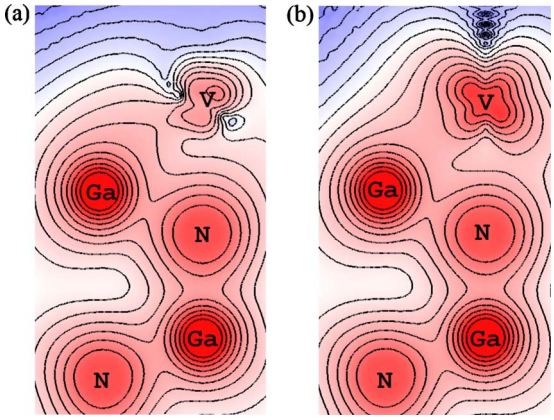

FIG. 8. (Color online) Cross-sectional view of the (a) minority-spin and (b) majority-spin charge densities for the V-T4 reconstruction. Red/dark colors represent larger charge-density values.

In the V-T4 reconstruction, the V adatom is near to three Ga surface atoms, and bonds with them, and therefore it saturates the dangling bonds. The total SMMC is about ~2.05μ_B (see Table II), and that value is a consequence of the high charge density of the majority spin located at the top of the V adatom. That fact can be observed in Fig. 7, where charge density is plotted as 2D diagram with lines of equal density. The V-T4 reconstruction evidences a small induced magnetization of the Ga atoms (in top layer) influenced by the local V adsorption. The vanadium adsorption results in a perturbation of the electronic properties mostly localized on the first layer. As far as the V states are concerned, we observe that their contribution to the occupied majority-spin component is by far larger than their contribution to the minority spin. The V local adsorption gives rise to a quite different surface electronic structure. In addition, we can see from the charge-density contours (Fig. 8) that the main spin magnetic moment per cell comes from the V atom.

In Fig. 7(c), we show the DOS for the V incorporation on the GaN(0001) surface in the configuration (4/0/0/). V-top-layer-projected DOS is also shown (red line). Compared with Fig. 7(a), the general feature of total states introduced by Ga-N sublayers is almost unchanged while the V impurities induce majority-spin states located at the top of the valence band and minority-spin states inside the conduction band. In the upper panel of Fig. 7(c), the Fermi level crosses the majority-spin level, suggesting a metallic state. These metallic states are mainly due to the V-top dangling bonds in the configuration (4/0/0). However, in the minority-spin DOS it is at the band gap without crossing any states, indicating an insulating state. Based on that observation, we can suggest a possible half-metallic behavior.

IV. CONCLUSIONS

Vanadium adsorption, diffusion, and incorporation on GaN(0001)-2×2 surface was studied using spin density-

functional theory. The V adatom adsorption was found to be most stable at T4 positions while the T1 position is an unfavorable site, even for different values of surface coverage ($\theta_V = 1/4$, 1/2, 3/4, and 1 ML). We found that the diffusion barrier from H3 toward T4 is about 0.18 eV and is 0.46 eV for the reverse path. This is an indication of a significant diffusion of V adatoms on the GaN(0001) surface. Our calculations show that the growth of monolayers of V atoms on this surface is possible. This is interesting from a theoretical point of view and for its technological applications. Using a thermodynamic approach, the calculated surfaces energies demonstrate that the vanadium atoms prefer one Ga substitution at the top bilayer and there appears to be no migration to the GaN bulk. We found that the incorporation of V in the GaN(0001) surface is most favorable under a nitrogen environment, in agreement with recent experimental results. From the calculated charge densities, we found a high majority-spin component concentration close to vanadium adatoms. Therefore, the main spin magnetic moment comes from vanadium atoms in the supercell.

ACKNOWLEDGMENTS

The calculations reported in this paper were performed using computing facilities of the HIPERLAB-cluster of Universidad del Norte, and the DGSCA-UNAM supercomputing center. The research published in this paper was partially supported by Universidad del Norte, DIB-Universidad Nacional de Colombia, and Conacyt under Grants No. 48549 and No. 89768, DGAPA-UNAM under Grant No. IN108908.

*rhernandezj@uninorte.edu.co
†jarodriguezm@bt.unal.edu.co

[1] S. Nakamura, Solid State Commun. **102**, 237 (1997).
[2] S. Nakamura, M. Senoh, N. Iwasa, and S. Nagahama, Appl. Phys. Lett. **67**, 1868 (1995).
[3] A. Hass Bar-Ilan, S. Zamir, O. Katz, B. Meyler, and J. Salzman, Mater. Sci. Eng., A **302**, 14 (2001).
[4] R. Trew, M. Shin, and V. Gatto, Solid-State Electron. **41**, 1561 (1997).
[5] S. Pearton, F. Ren, A. Zhang, and K. Lee, Mater. Sci. Eng. R. **30**, 55 (2000).
[6] T. Dietl, H. Ohno, F. Matsukura, J. Cibert, and D. Ferrand, Science **287**, 1019 (2000).
[7] T. Jungwirth, J. Sinova, J. Masek, J. Kucera, and A. H. MacDonald, Rev. Mod. Phys. **78**, 809 (2006).
[8] L. Kronik, M. Jain, and J. R. Chelikowsky, Phys. Rev. B **66**, 041203(R) (2002).
[9] K. Sato, P. Dederics, and H. Katayama-Yoshida, Europhys. Lett. **61**, 403 (2003).
[10] N. Tandon, G. P. Das, and A. Kshirsagar, Phys. Rev. B **77**, 205206 (2008).
[11] M. Souissi, A. Bchetnia, and B. E. Jani, J. Cryst. Growth **277**, 57 (2005).
[12] H. Touati, M. Souissi, Z. Chine, and B. El Jani, Microelectron. J. **39**, 1457 (2008).
[13] M. Souissi, H. Touati, A. F. A. Bchetnia, and B. E. Jani, Microelectron. J. **39**, 1521 (2008).
[14] J. S. Lee, J. D. Lim, Z. G. Khim, Y. D. Park, S. J. Pearton, and S. N. G. Chu, J. Appl. Phys. **93**, 4512 (2003).
[15] V. A. Guzenko, N. Thillosen, A. Dahmen, R. Calarco, T. Schapers, L. Houben, M. Luysberg, B. Schineller, M. Heuken, and A. Kaluza, J. Appl. Phys. **96**, 5663 (2004).
[16] R. González Hernández, W. Lopez, F. Fajardo, and J. A. Rodriguez, Mater. Sci. Eng., B **163**, 190 (2009).
[17] C. K. Ramesh, V. R. Reddy, and K. S. R. K. Rao, J. Mater. Sci.: Mater. Electron. **17**, 999 (2006).
[18] C. O. López, W. L. Pérez, and J. A. Rodriguez M., Appl. Surf. Sci. **255**, 3837 (2009).
[19] T. Zywietz, J. Neugebauer, and M. Scheffler, Appl. Phys. Lett. **73**, 487 (1998).
[20] T. Zywietz, J. Neugebauer, M. Scheffler, J. Northrup, and C. G. V. de Walle, MRS Internet J. Nitride Semicond. Res. **3**, 26 (1998).
[21] C. G. Van de Walle and J. Neugebauer, Phys. Rev. Lett. **88**, 066103 (2002).
[22] Q. Z. Xue, Q. K. Xue, R. Z. Bakhtizin, Y. Hasegawa, I. S. T. Tsong, T. Sakurai, and T. Ohno, Phys. Rev. B **59**, 12604 (1999).
[23] A. R. Smith, R. M. Feenstra, D. W. Greve, M. S. Shin, M. Skowronski, J. Neugebauer, and J. E. Northrup, Surf. Sci. **423**, 70 (1999).
[24] Q. K. Xue, Q. Z. Xue, R. Z. Bakhtizin, Y. Hasegawa, I. S. T. Tsong, T. Sakurai, and T. Ohno, Phys. Rev. Lett. **82**, 3074 (1999).
[25] J. P. Perdew, K. Burke, and M. Ernzerhof, Phys. Rev. Lett. **77**, 3865 (1996).
[26] K. Laasonen, A. Pasquarello, R. Car, C. Lee, and D. Vanderbilt, Phys. Rev. B **47**, 10142 (1993).
[27] P. Giannozzi *et al.*, J. Phys.: Condens. Matter **21**, 395502 (2009); http://www.quantum-espresso.org
[28] H. Monkhorst and J. Pack, Phys. Rev. B **13**, 5188 (1976).
[29] M. Methfessel and A. T. Paxton, Phys. Rev. B **40**, 3616 (1989).
[30] K. Kim, W. R. L. Lambrecht, and B. Segall, Phys. Rev. B **53**, 16310 (1996).
[31] C. Stampfl and C. G. Van de Walle, Phys. Rev. B **59**, 5521 (1999).
[32] M. Bernasconi, G. L. Chiarotti, and E. Tosatti, Phys. Rev. B **52**, 9988 (1995).
[33] J. E. Northrup, R. Di Felice, and J. Neugebauer, Phys. Rev. B **55**, 13878 (1997).
[34] D. R. Lide, *Handbook of Chemistry and Physics* (CRC Press, Boca Raton, Florida, 1995).
[35] A. T. Paxton, M. Methfessel, and H. M. Polatoglou, Phys. Rev. B **41**, 8127 (1990).
[36] M. Fuchs, J. L. F. Da Silva, C. Stampfl, J. Neugebauer, and M. Scheffler, Phys. Rev. B **65**, 245212 (2002).
[37] R. C. Powell, N. E. Lee, Y. W. Kim, and J. E. Greene, J. Appl. Phys. **73**, 189 (1993).
[38] T. J. Peshek, J. C. Angus, and K. Kash, J. Cryst. Growth **311**, 185 (2008).
[39] A. R. Smith, R. M. Feenstra, D. W. Greve, J. Neugebauer, and J.

E. Northrup, Phys. Rev. Lett. **79**, 3934 (1997).
[40] T. Strasser, C. Solterbeck, F. Starrost, and W. Schattke, Phys. Rev. B **60**, 11577 (1999).
[41] A. L. Rosa and J. Neugebauer, Phys. Rev. B **73**, 205346 (2006).
[42] F. H. Wang, P. Krüger, and J. Pollmann, Phys. Rev. B **64**, 035305 (2001).
[43] N. Takeuchi, A. Selloni, T. H. Myers, and A. Doolittle, Phys. Rev. B **72**, 115307 (2005).
[44] C. Bungaro, K. Rapcewicz, and J. Bernholc, Phys. Rev. B **59**, 9771 (1999).
[45] A. L. Rosa and J. Neugebauer, Phys. Rev. B **73**, 205314 (2006).
[46] S. Pookpanratana, R. France, M. Bar, L. Weinhardt, O. Fuchs, M. Blum, W. Yang, J. D. Denlinger, T. D. Moustakas, and C. Heske, Appl. Phys. Lett. **93**, 172106 (2008).
[47] Q. Sun, A. Selloni, T. H. Myers, and W. A. Doolittle, Phys. Rev. B **73**, 155337 (2006).
[48] G.-X. Qian, R. M. Martin, and D. J. Chadi, Phys. Rev. B **38**, 7649 (1988).
[49] D. Segev and C. G. V. de Walle, J. Cryst. Growth **300**, 199 (2007).
[50] J. E. Northrup, J. Neugebauer, R. M. Feenstra, and A. R. Smith, Phys. Rev. B **61**, 9932 (2000).